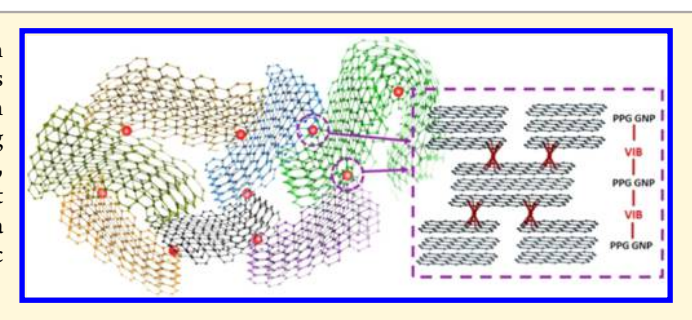


Application of Organometallic Chemistry to the Electrical Interconnection of Graphene Nanoplatelets

Mingguang Chen, $^{\dagger,\$}$ Xiaojuan Tian, $^{\dagger,\$}$ Wangxiang Li, $^{\dagger,\$}$ Elena Bekyarova, $^{\ddagger,\$}$ Guanghui Li, $^{\dagger,\$}$ Matthew Moser, $^{\ddagger,\$}$ and Robert C. Haddon $^{*,\dagger,\pm,\$}$

Supporting Information

ABSTRACT: The formation of bis-hexahapto bonds between graphitic surfaces can electronically interconnect the surfaces of carbon materials containing the polybenzenoid ring system and increase the conductivity without introducing a strong perturbation to the in-plane electronic structure. In this paper, we report the use of organometallic chemistry to interconnect the surfaces of small scale graphene nanoplatelets by using a variety of metals and photochemically activated organometallic reagents.



INTRODUCTION

Graphene has received a great deal of attention in recent years, ¹ with anticipated applications in material science, biotechnology,³ electronics,⁴⁻⁷ and spintronics.⁸ Furthermore, the interaction between metals and graphene surfaces has long been a popular topic. 9-14 In fact, bulk materials composed of single-layer graphene (SLG) sheets have been known for many years, as exemplified by the stage 1 graphite intercalation compounds (GICs) such as KC8; similarly the stage 2 GICs contain bilayer graphene, and this continues up to at least the stage 4 compounds. 15 Recently, we have pursued the organometallic chemistry of the tricoordinate conjugated carbon allotropes 16-18 with particular emphasis on carbon nanotubes, and we have shown that the formation of covalent bis(η^6 -SWNT)M bonds is an effective way to interconnect the junctions of the SWNTs in thin films and leads to an enhanced electrical conductivity in the case of some of the first row transition metals (Ti, V, Cr, Mn, Fe), 19 the group 6 metals (Cr, Mo, W),²⁰ and the lanthanides (La, Nd, Sm, Eu, Gd, Dy, Ho, Yb). 21,22 It would be expected that the same chemistry could be applied to the insertion of transition metals between pairs of parallel graphene surfaces to generate compounds analogous to the GICs in which the ionic bonds characteristic of the GICs are replaced by covalent bis-hexahapto bonds, 18 and there is strong theoretical evidence for this mode of bonding.^{23–27} We have pursued the hexahapto-graphene compounds in solution phase 16,28 and in solid state 29 reactions, but the compounds cannot be prepared by the routes usually employed for the synthesis of GICs because of the absence of charge transfer in the transition metal complexes.³⁰

Graphene nanoplatelets (GNPs) are a particularly attractive material for a number of applications due to their large scale

production, and the availability of simple routes to solutionbased and film-based material forms. 31-34 We previously explored the use of organometallic chemistry to enhance the conductivity of exfoliated GNPs by thermal processing under pressure, but this was not successful, perhaps due to the large particle sizes and the exposure of the samples to the atmosphere during the preparation. 29,33 In the present manuscript, we explore the organometallic chemistry of a new form of GNPs prepared by PPG Industries (http:// corporate.ppg.com/Home.aspx) (PPG GNPs) in which the size of the GNPs is much smaller than that of the conventional exfoliated GNPs prepared from natural graphite. The PPG material possesses a crinkled morphology which should facilitate the interconnection of the graphene surfaces of different PPG GNPs and allow the formation of bis-hexahapto bonds between adjoining graphene surfaces within distorted individual PPG GNPs, thereby facilitating the formation of a novel 3D-connected material, as shown in Figure 1. Thus, it may be possible to conserve the extraordinary physical and chemical properties of graphene in the in-plane direction, while interconnecting and improving the interactions between adjacent GNP sheets by the formation of bis-hexahapto covalent bonds in the orthogonal directions, throughout the solid material (Figure 1).

We make use of metal vapor synthesis (MVS)^{19,30} and photochemical³⁵ routes for the preparation of the transition metal complexes which are carried out in a vacuum and in the

Received: January 17, 2016 Revised: March 11, 2016 Published: March 12, 2016



Department of Chemical and Environmental Engineering, University of California, Riverside, California 92521, United States

Department of Chemistry, University of California, Riverside, California 92521, United States

[§]Center for Nanoscale Science and Engineering, University of California, Riverside, California 92521, United States

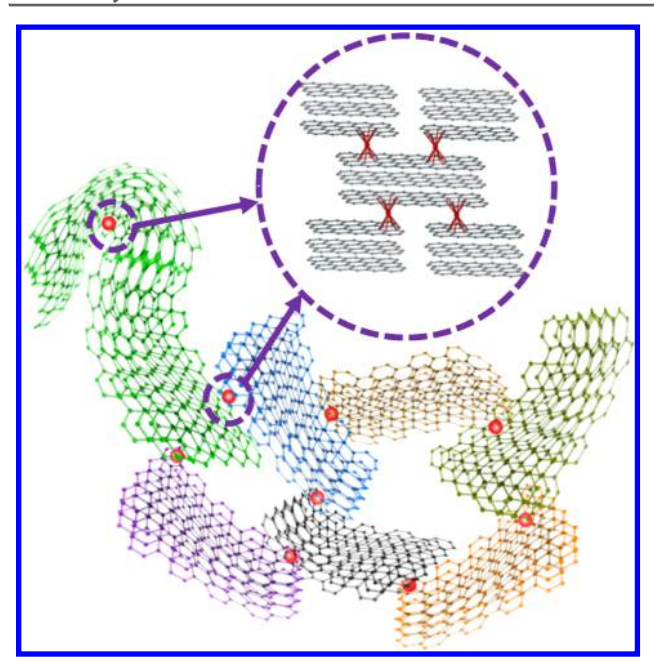


Figure 1. Schematic of the formation of metal complexes with the surface of PPG GNPs. Different colors of PPG GNPs represent different nanoparticles.

atmosphere of a glovebox, respectively, while the conductivities of the thin films of PPG GNPs are monitored in situ.

■ RESULTS AND DISCUSSION

PPG GNPs. The PPG GNP material is synthesized from methane in a gas phase, continuous plasma process,³⁶ and below, we report some of our characterization studies of this new material.

We carried out atomic force microscopy (AFM) measurements to characterize the lateral dimensions and thickness of the PPG GNPs. Figure 2 shows that the lateral size of the PPG GNPs varies from 50 to 500 nm, and the thickness is in the range from 2 to 50 nm, which corresponds to 6–150 layers of graphene.

Scanning electron microscopy (SEM) was employed to study the morphology of PPG GNPs, and the SEM image in Figure 3 indicates that the PPG GNPs have a crinkled morphology which distinguishes this material from traditional graphene nanoplatelets. Of particular importance in the present application is the relatively small size of the nanoplatelets in comparison to standard GNPs obtained from the exfoliation of natural graphite; furthermore, the size distribution of the PPG GNPs is narrower than that in the traditional materials.³³

A representative Raman spectrum of the PPG GNPs is compared with other forms of graphene in Figure 4. The Raman spectrum shows a G-peak at ~1567 cm⁻¹ and an intense 2D-peak at ~2678 cm⁻¹, which indicates a graphene-like electronic structure. The relatively strong D-peak in the PPG GNPs probably originates from the small flake size: on the basis of literature analyses of the flake dimensions as a function of the Raman $I_{\rm D}/I_{\rm G}$ ratio, ^{37,38} we estimate a particle size for PPG GNPs of 0.5 μ m which is a little larger than that obtained from the AFM measurements. The shape of the 2D-peak is a single Lorentzian, and the intensity of G-peak is smaller than that of the 2D-peak, similar to single layer graphene, which suggests that the layers of the PPG GNP sample are not Bernal-stacked but are rotationally disordered much like in the case of

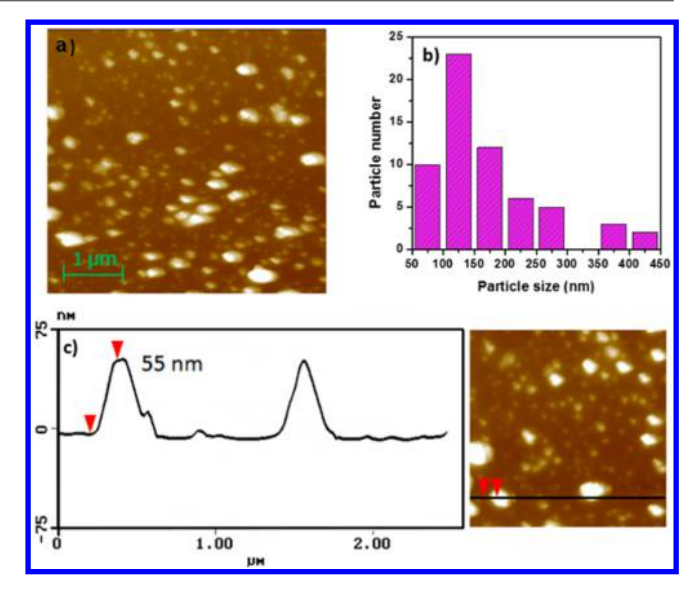


Figure 2. (a) AFM image of PPG GNPs previously dispersed in orthodichlorobenzene. (b) Distribution of the PPG GNPs by lateral size. (c) AFM analysis of nanoparticle thickness.

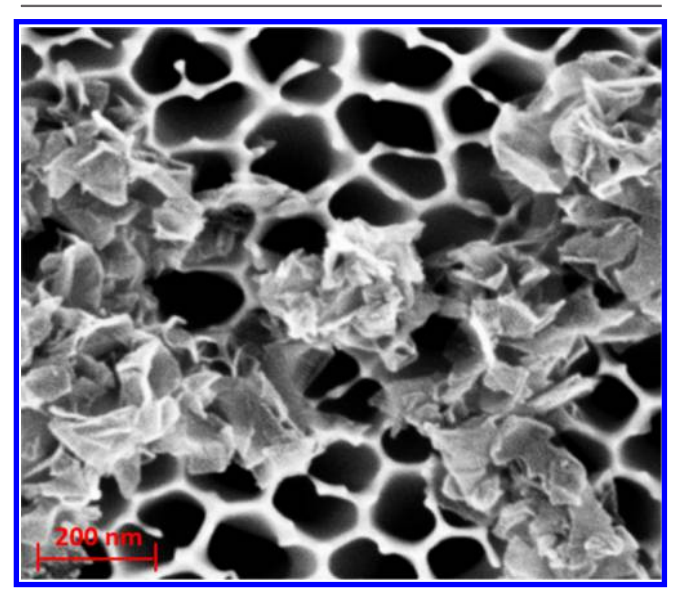


Figure 3. SEM image of PPG GNPs at an areal density of 5 mg/cm² on an Al_2O_3 filter membrane.

epitaxial graphene.^{39,40} The disorder between graphene layers minimizes the electronic interaction between the sheets and preserves the single graphene sheet properties of the layers.

PPG GNP Film Formation. Thin films were prepared by spraying tetrahydrofuran (THF) dispersed PPG GNPs onto glass substrates with prepatterned electrodes, as shown in the microscope images of our pristine samples (Figure 5). There is some restacking of the PPG GNP particles on the substrate, but in general, the PPG GNP material does not seem to reaggregate to the same degree as other GNPs and reasonably uniform thin films can be obtained. Figure 5c shows the cross-sectional profile obtained by use of a Dektak Profilometer for a typical PPG GNP thin film used in our experiments (thickness ≈ 100 nm). These films are of comparable thickness to the particle dimensions, and thus, they retain characteristics of a percolating network which makes them sensitive to the quality of the inter-GNP junctions.³⁰

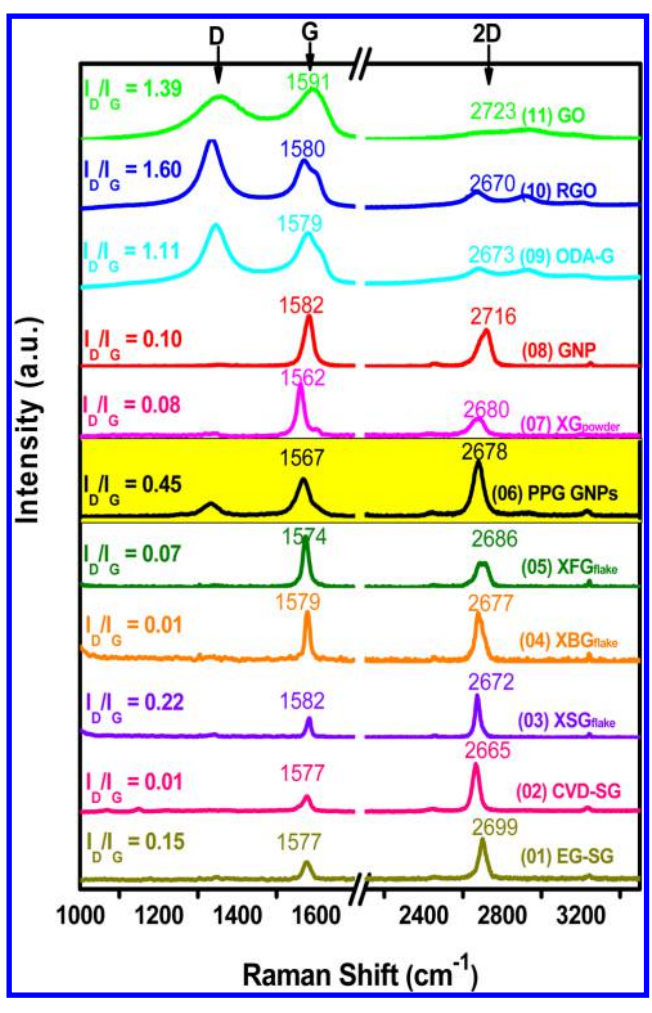


Figure 4. Raman spectra of PPG GNPs in comparison with other forms of graphene.

In order to better understand the properties of PPG GNP thin film, UV–vis–NIR spectra were taken on our solid films on glass substrates (Figure 6). The spectra show well-defined slopes in the short wavelength region of the spectrum, which is characteristic of nanomaterials such as graphene or single-walled carbon nanotubes (SWNTs) that typically show a peak at \sim 270 nm, corresponding to the $\pi \to \pi^*$ transitions within the graphene sheets. The extinction coefficient of PPG GNPs

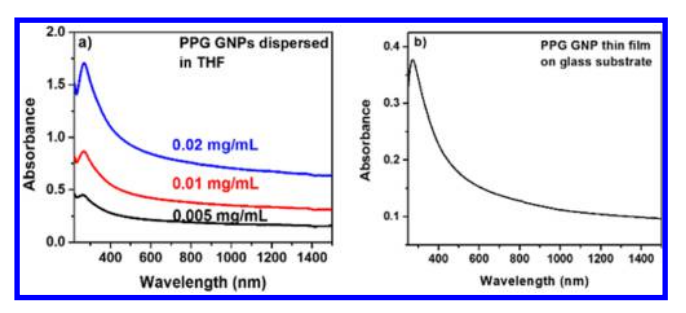


Figure 6. UV-vis-NIR spectra of (a) PPG GNPs dispersed in THF as a function of concentration and (b) PPG GNP film (100 nm) versus wavelength.

dispersed in THF calculated from Figure 6a at 660 nm is $\varepsilon=48$ L·g⁻¹·cm⁻¹, and the absorbance coefficient of the PPG GNP thin film calculated from Figure 6b is $\alpha=0.32\times10^5$ cm⁻¹ (660 nm). On the basis of our previous analysis and the absorption characteristics of the materials, ⁴¹ we can calculate an effective density for the film of d=0.29 g cm⁻³; as expected, thicker films have higher densities (typically, $d\approx0.77$ g cm⁻³). The AFM image of the PPG GNP thin film is shown in Figure 7, which indicates that the PPG GNP particles flocculate during the spraying process, thereby leading to a loosely packed structure.

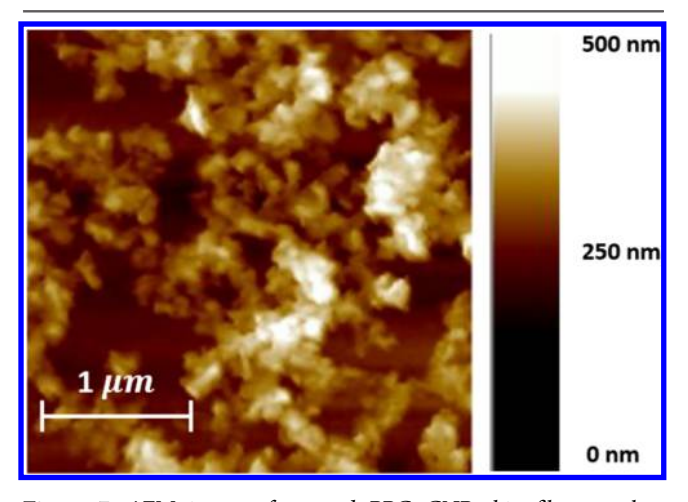


Figure 7. AFM image of sprayed PPG GNP thin film on glass substrate.

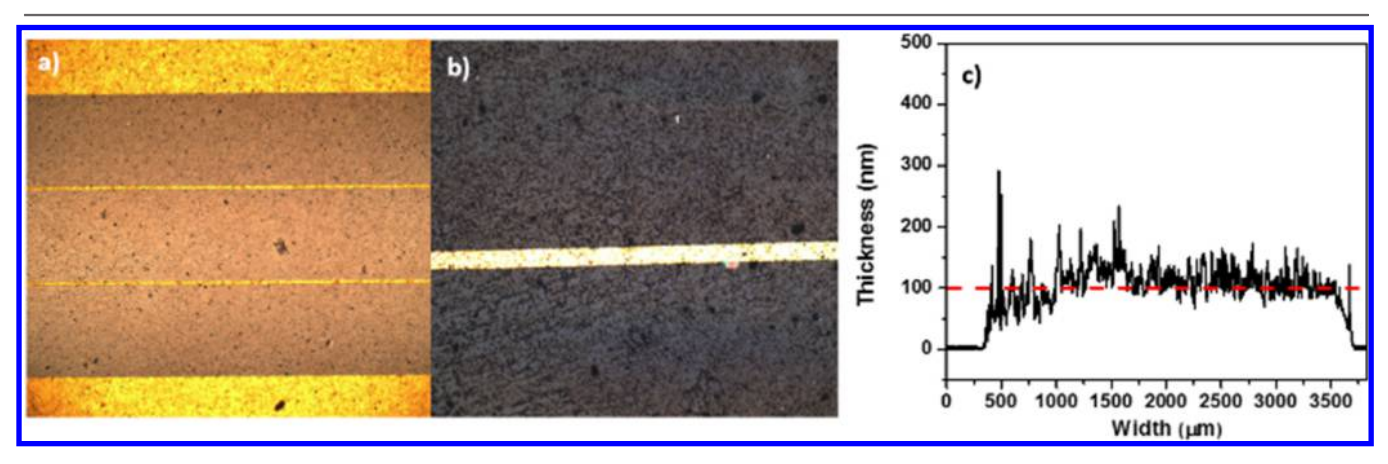


Figure 5. Microscope images of sprayed PPG GNP thin film at magnifications: (a) 100×; (b) 500×. (c) Dektak profilometer cross-sectional characterization of a typical PPG GNP thin film.

Response of the PPG GNP Thin Film Conductivities to Metal Deposition and Photochemical Reaction with Organometallic Precursors. Before exposure of the PPG GNP films to the metals and organometallic reagents, the pristine thin film samples were annealed at 300 °C in a vacuum for 5 h just before conducting the reaction in order to remove solvents and volatile dopants. Figure 8 shows schematics of the

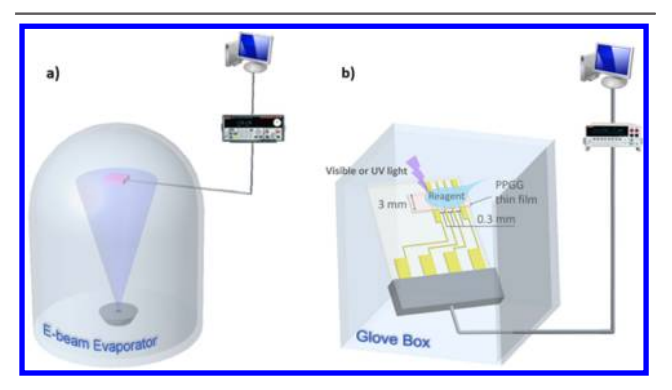


Figure 8. Schematics of the experimental organometallic conductivity configurations: (a) metal vapor synthesis (MVS) conducted in a Temescal high vacuum E-beam evaporator; (b) photochemical reaction conducted in a glovebox.

experimental setups employed in the MVS and photochemical experiments. For the MVS method, ^{19,30} metal sources are loaded in the hearth of the electron beam chamber, and for the photochemical method, the various metal derivatives are dissolved in acetonitrile.³⁵ In situ measurements are conducted by use of prewired electrical harnesses connecting the samples inside the E-beam chamber or the glovebox using feed throughs to interface with a computer controlled Keithley 2700 multichannel meter. Single layer CVD graphene (SLG) was first used to benchmark the interaction between a graphene surface and the bare transition metal chromium (Cr). Figure 9a

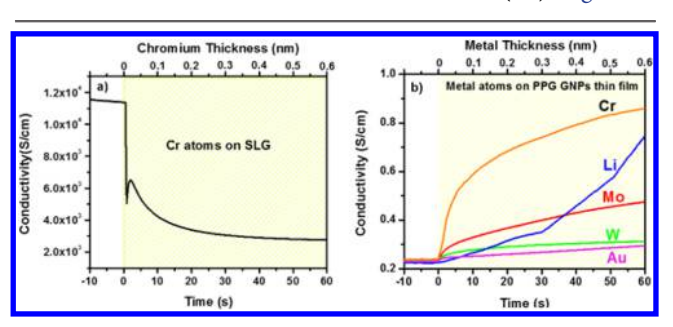


Figure 9. Conductivities of thin films on metal atom deposition from an E-beam evaporator: (a) transferred single layer CVD graphene as a function of metal thickness; (b) conductivity of PPG GNP films as a function of metal deposition.

shows that, after evaporating 0.6 nm Cr on the top surface of transferred SLG on a glass substrate, the conductivity of SLG decreased from $\sigma = 1.15 \times 10^4$ S/cm to $\sigma = 4 \times 10^3$ S/cm, which is probably due to electron scattering from the Cr atoms on the surface of graphene. STM experiments indicate that Cr atoms are mobile on graphene surfaces and are attracted to defects and contaminants, and the formation of clusters has been observed on graphitic surfaces and carbon nanotubes. 20,42,43 In general, metals interact with graphitic surfaces in three distinct modalities: (a) physisorption in which there is minimal charge transfer or bonding, (b) chemisorption in

which there are ionic bonding and charge transfer from the metal, and (c) covalent chemisorption in which there is appreciable rehybridization of the graphitic electronic structure. We have recently distinguished a fourth mode, (d), in which there is bis-hexahapto bonding to the graphitic surface with minimal rehybridization. 18 Thus, for the present study, we chose metals to represent classes: (a) Au, (b) Li, and (d) Cr, Mo, and W, in our studies of the PPG GNP films; the results of evaporating 0.6 nm of these metals on the surfaces of the PPG GNP films are shown in Figure 9b. The results for Au show a very weak effect, as expected for physisorption (a), in which there is the formation of a parallel conducting film. Previous studies indicate a very weak interaction between gold and graphitic surfaces. 12-14,19 Lithium shows clear evidence of charge transfer with donation of electrons into the conduction band of the PPG GNPs and a strongly enhanced conductivity, providing clear evidence for mechanism (b), ionic chemisorption or doping. When 0.6 nm of Cr atoms was evaporated onto the PPG GNP thin films, the conductivity of the films increased from $\sigma = 0.22$ S/cm to 0.82 S/cm, which contrasts with the result obtained on evaporation of Cr on SLG sheets (above). In the present instance, it appears that the Cr atoms are able to bridge some of the nanoplatelets and to spontaneously form covalent bis $(\eta^6$ -GNP)Cr bonds that enhance the conductivity. The observed conductivity enhancement amounts to about a factor of 3-4 which is very similar to the values observed on deposition of Cr on metallic (MT)-SWNT films.³⁰ The evaporation of the other group 6 metals, molybdenum (Mo) and tungsten (W), onto the PPG GNP films also enhances the conductivities, but the increases in conductivity are much more modest. We previously found the same behavior with SWNT films, and we ascribed the weaker effect of the larger group 6 metals to the difficulty of inserting these atoms between the graphitic surfaces.²⁰ In Figure 10, we show the effect of irradiating the PPG GNP films after treatment with organometallic reagents; the lower traces of Figure 10a show the effect of the reagent alone and of a blank irradiation experiment. It is clear that the simultaneous application of the reagent together with UVC (254 nm) light is necessary to initiate the reaction. As may be seen in Figure 10a, irradiation with UVC light in the presence of $Cr(CO)_6$ leads to an increase in the conductivity of the PPG GNP thin film from $\sigma = 0.22$ S/cm to 0.9 S/cm, which is consistent with the MVS results. It is also clear that the same mechanism operates in the case of GNP and the SWNT films.³⁵ Figure 10b compares the reactivity of the various chromium reagents with the PPG GNP films, and it is apparent that the order of reactivity follows the sequence $Cr(CO)_6 < Cr(\eta^6$ -benzene) $(CO)_3 < Cr(\eta^6$ -benzene)₂. Nevertheless, the final conductivities are very close and it is apparent that the same final material composition is achieved irrespective of the organometallic reagent. The Mo(CO)₆ and W(CO)₆ reagents also react with the PPG GNP thin films under UVC light, but the final conductivities are less than in the case of the Cr compounds (Figure 10c).

The final conductivities of the new 3D cross-linked GNP materials synthesized by the photochemical route are fully consistent with those made by the MVS method (Figure 11), which adds further support to our proposed mechanism. To the best of our knowledge, this is the first report of new 3D graphene materials obtained from GNPs by constructive covalent bonding accompanied by an enhancement of the bulk electrical conductivity.

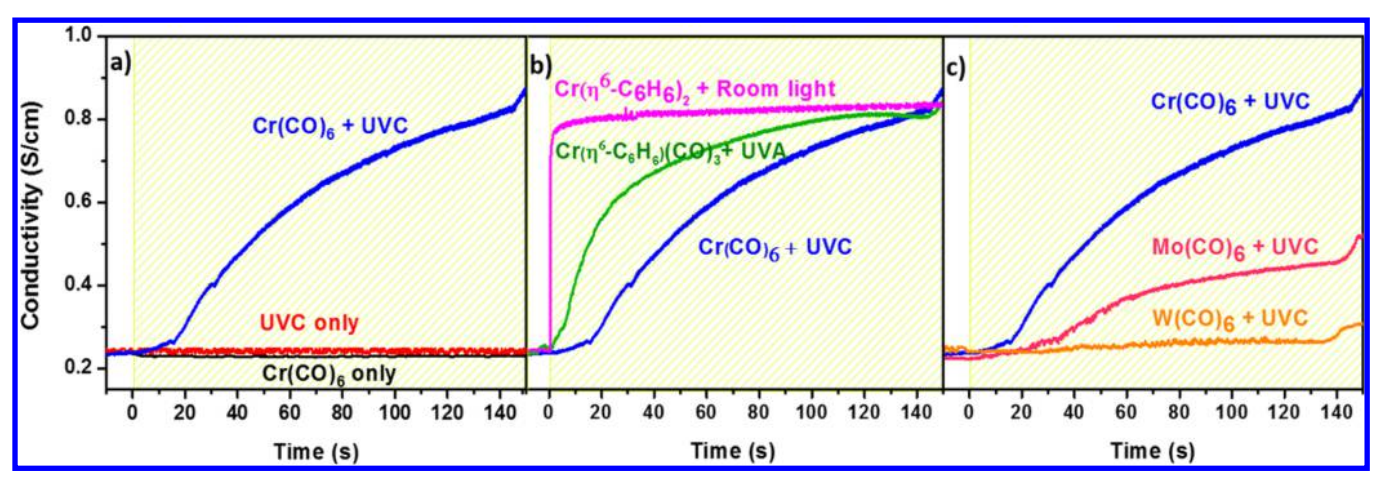


Figure 10. Evolution of PPG GNP thin film conductivities on photochemical reaction with organometallic reagents.

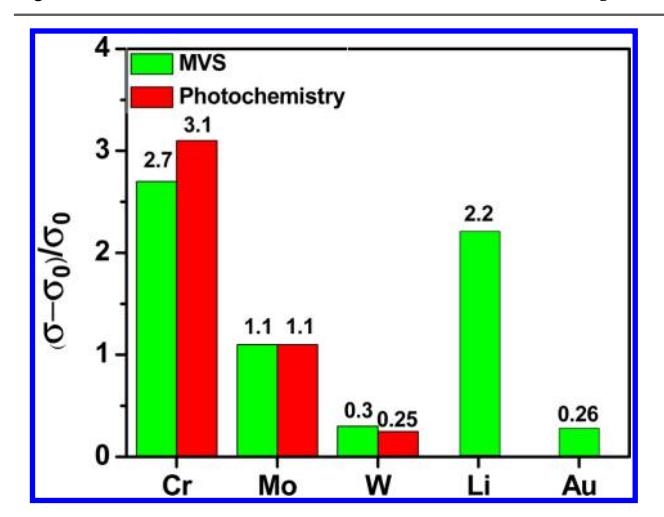


Figure 11. Conductivity enhancements of various metal complexes formed with PPG GNP thin films by MVS and by photochemistry of organometallic reagents.

CONCLUSION

In conclusion, we were able to cross-link bulk PPG GNPs by use of group 6 transition metals using metal vapor synthesis and the photoinduced reactions of organometallic reagents. The new 3D-interconnected graphene materials show enhanced electrical conductivities, and thus, it is possible to interconnect the graphene sheets without grossly interfering with the extraordinary properties of graphene. The reactivity of the organometallic chromium reagents with PPG GNPs follows the same order that was found with single-walled carbon nanotubes: $Cr(CO)_6 < Cr(\eta^6$ -benzene) $(CO)_3 < Cr(\eta^6$ benzene)2. The effectiveness of the group 6 transition metals in increasing the conductivity of GNP films is in the following order: W < Mo < Cr. These novel 3D graphene materials are of potential interest in catalysis, electronics, and spintronics. 17,24,25 This study encourages the pursuit of a 3D graphene formed by introducing transition metals between single graphene layers in analogy with the GIC compounds but in which the ionic interactions are replaced by covalent $\mathrm{Cr}(\eta^6\text{-graphene})_2$ bonding. 16,17

■ EXPERIMENTAL SECTION

Exfoliated Graphene (XG). For the Raman spectroscopy, XG was exfoliated by the scotch tape method⁴⁴ from highly oriented pyrolytic graphite (HOPG) (Union Carbide Corporation, grade ZYH).

Epitaxial Graphene (EG). For the Raman spectroscopy, EG was grown on the C-face of a SiC substrate (Cree Inc., high purity) and was obtained from the de Heer group (Georgia Tech).

Single Layer Graphene Transfer. Single layer graphene grown by chemical vapor synthesis on copper (Graphene Supermarket) was transferred onto glass substrates using literature methods.⁴⁵

PPG GNP Thin Film Preparation. PPG GNP powders (obtained from PPG Industries) were dispersed in tetrahydrofuran (THF) at a concentration of 0.03 mg/mL; the dispersion was then sonicated for 1 h (VWR Ultrasonic Cleaner, model no. 75T). Then, the solution was sprayed onto a glass substrate with prepatterned electrodes at 70 °C. For conductivity measurement, the samples were annealed in a vacuum for 5 h at 300 °C in order to remove atmospheric dopants.

Metal Vapor Synthesis (MVS). After vacuum annealing, the samples were transferred into a cryopumped Temescal BJD 1800 Ebeam evaporator and the system pumped for 10 h until the vacuum inside the chamber had reached 8×10^{-7} Torr.

Photochemistry. Solutions of Mo(CO)₆ (Sigma-Aldrich 98%) and W(CO)₆ (Alfa Aesar 97%) were prepared in degassed acetonitrile inside a glovebox at a concentration of 1×10^{-3} M. The protocol for the chromium organometallics is described in a previous paper.³⁵ We employed the following light sources: Cr(CO)₆, Mo(CO)₆ and W(CO)₆ [UVC, 254 nm], Cr(η^6 -benzene) (CO)₃ [UVA, 365 nm], Cr(η^6 -benzene)₂ [room light].

Conductivity Measurement. The samples were interfaced with a computer controlled Keithley 2700 model 7708 Differential Multiplexer by use of feed troughs and wire harnesses.

SEM. PPG GNPs were dispersed in dimethylformamide (DMF) in sufficient concentration to make samples of areal density 5 μ g/cm² after filtration through an Al₂O₃ membrane (Whatman 0.02 μ m). Pt/Pd was sputtered on the surface of the sample before conducting the GeminiSEM study.

Raman Spectroscopy. Raman spectra were acquired with a Nicolet Almega XR Dispersive Raman microscope using 532 nm laser excitation and 25% power source.

Optical Microscopy. Optical microscope images of sprayed PPG thin film samples were obtained with an Olympus BX51W1 microscope.

Measurement of Film Thickness. Cross-sectional profiles for thin film samples were obtained with a Dektak Profilometer.

UV-vis-NIR Spectroscopy. Absorption spectra of 0.03 mg/mL THF dispersions of PPG graphene nanoparticles were collected utilizing a Varian Cary 5000 spectrophotometer. The absorption spectra were measured using cuvettes of 2 mm light path length. The dispersions were prepared by 1 h of sonication (VWR Ultrasonic Cleaner, model no. 75T).

AFM. PPG GNP powders were dispersed in ortho-dichlorobenzene by ultrasonication (VWR Aquasonic HT250 bath sonicator) for 20 min. A drop of the dispersion was placed on a mica substrate and allowed to dry, and the images were collected in tapping mode (Digital

Instruments, MMAFM-2). For the PPG GNP thin films, a Dimension 3100 Nanoman Veeco AFM was employed to characterize the morphology with a golden silicon probe (NT-MDT, NSG01), and the images were obtained in tapping mode.

ASSOCIATED CONTENT

S Supporting Information

The Supporting Information is available free of charge on the ACS Publications website at DOI: 10.1021/acs.chemmater.6b00217.

Abbreviations and analysis of the effect of film thickness on photochemistry reaction (PDF)

AUTHOR INFORMATION

Corresponding Author

*E-mail: haddon@ucr.edu.

Notes

The authors declare no competing financial interest.

ACKNOWLEDGMENTS

This work was funded by PPG Industries Inc (studies of PPG GNP material) and by NSF under contract DMR-1305724 (organometallic chemistry).

REFERENCES

- (1) Geim, A. K.; Novoselov, K. S. The Rise of Graphene. *Nat. Mater.* **2007**, *6*, 183–191.
- (2) Sarkar, S.; Bekyarova, E.; Niyogi, S.; Haddon, R. C. Diels-Alder Chemistry of Graphite and Graphene: Graphene as Diene and Dienophile. *J. Am. Chem. Soc.* **2011**, *133*, 3324–3327.
- (3) Wang, Y.; Li, Z.; Wang, J.; Li, J.; Lin, Y. Graphene and Graphene Oxide: Biofunctionalization and Applications in Biotechnology. *Trends Biotechnol.* **2011**, *29*, 205–212.
- (4) Berger, C.; Song, Z.; Li, T.; Li, X.; Ogbazghi, A. Y.; Feng, R.; Dai, Z.; Marchenkov, A. N.; Conrad, E. H.; First, P. N.; de Heer, W. A. Ultrathin Epitaxial Graphite: 2D Electron Gas Properties and a Route Toward Graphene-Based Nanoelectronics. *J. Phys. Chem. B* **2004**, *108*, 19912–19916.
- (5) Chen, Z. H.; Lin, Y. M.; Rooks, M. J.; Avouris, P. Graphene Nano-Ribbon Electronics. *Phys. E* **2007**, *40*, 228–232.
- (6) Liu, C.-H.; Chang, Y.-C.; Norris, T. E.; Zhong, Z. Graphene Photodetectors with Ultra-Broadband and High Responsivity at Room Temperature. *Nat. Nanotechnol.* **2014**, *9*, 273–278.
- (7) Torrisi, F.; Hasan, T.; Wu, W. P.; Sun, Z. P.; Lombardo, A.; Kulmala, T. S.; Hsieh, G. W.; Jung, S. J.; Bonaccorso, F.; Paul, P. J.; Chu, D. P.; Ferrari, A. C. Inkjet-Printed Graphene Electronics. ACS Nano 2012, 6, 2992–3006.
- (8) Nair, R. R.; Sepioni, M.; Tsai, I.-L.; Lehtinen, P. O.; Keinonen, J.; Krasheninnikov, A. V.; Thomson, T.; Geim, A. K.; Grigorieva, I. V. Spin-Half Paramagnetism in Graphene Induced by Point Defects. *Nat. Phys.* **2012**, *8*, 199–202.
- (9) Charlier, J. C.; Arnaud, L.; Avilov, I. V.; Delgado, M.; Demoisson, F.; Espinosa, E. H.; Ewels, C. P.; Felten, A.; Guillot, J.; Ionescu, R.; Leghrib, R.; Llobet, E.; Mansour, A.; Migeon, H. N.; Pireaux, J. J.; Reniers, F.; Suarez-Martinez, I.; Watson, G. E.; Zanolli, Z. Carbon Nanotubes Randomly Decorated with Gold Clusters: from Nano(2)-hybrid Atomic Structures to Gas Sensing Prototypes. *Nanotechnology* **2009**, *20*, 375501.
- (10) Sargolzaei, M.; Gudarzi, F. Magnetic Properties of Single 3d Transition Metals Adsorbed on Graphene and Benzene: A Density Functional Theory Study. *J. Appl. Phys.* **2011**, *110*, 064303.
- (11) Sevincli, H.; Topsakal, M.; Durgun, E.; Ciraci, S. Electronic and Magnetic Properties of 3d Transition-Metal Atom Adsorbed Graphene and Graphene Nanoribbons. *Phys. Rev. B: Condens. Matter Mater. Phys.* **2008**, *77*, 195434.

(12) Chan, K. T.; Neaton, J. B.; Cohen, M. L. First-Principles Study of Adatom Adsorption on Graphene. *Phys. Rev. B: Condens. Matter Mater. Phys.* **2008**, *77*, 235430.

- (13) Zan, R.; Bangert, U.; Ramasse, Q.; Novoselov, K. S. Metal-Graphene Interaction Studied via Atomic Resolution Scanning Transmission Electron Microscopy. *Nano Lett.* **2011**, *11*, 1087–1092.
- (14) Liu, X.; Wang, C.-Z.; Hupalo, M.; Lin, H.-Q.; Ho, K.-M.; Tringides, M. C. Metals on Graphene: Interactions, Growth Morphology, and Thermal Stability. *Crystals* **2013**, *3*, 79–111.
- (15) Dresselhaus, M. S.; Dresselhaus, G. Intercalation compounds of graphite. In *Advances in Physics*; Martin, D. H., Ed.; Taylor & Francis Ltd: London, 1981; Vol. 30, pp 139–326.
- (16) Sarkar, S.; Niyogi, S.; Bekyarova, E.; Haddon, R. C. Organometallic Chemistry of Extended Periodic π-Electron Systems: Hexahapto-Chromium Complexes of Graphene and Single-Walled Carbon Nanotubes. *Chem. Sci.* **2011**, *2*, 1326–1333.
- (17) Sarkar, S.; Moser, M. L.; Tian, X.; Zhang, X. J.; Al-Hadeethi, Y. F.; Haddon, R. C. Metals on Graphene and Carbon Nanotube Surfaces: From Mobile Atoms to Atomtronics to Bulk Metals to Clusters and Catalysts. *Chem. Mater.* **2014**, *26*, 184–195.
- (18) Bekyarova, E.; Sarkar, S.; Wang, F.; Itkis, M. E.; Kalinina, I.; Tian, X.; Haddon, R. C. Effect of Covalent Chemistry on the Electronic Structure and Properties of Carbon Nanotubes and Graphene. *Acc. Chem. Res.* **2013**, *46*, 65–76.
- (19) Wang, F.; Itkis, M. E.; Bekyarova, E.; Tian, X.; Sarkar, S.; Pekker, A.; Kalinina, I.; Moser, M.; Haddon, R. C. Effect of First Row Transition Metals on the Conductivity of Semiconducting Single-Walled Carbon Nanotube Networks. *Appl. Phys. Lett.* **2012**, *100*, 223111.
- (20) Kalinina, I.; Bekyarova, E.; Sarkar, S.; Wang, F.; Itkis, M. E.; Tian, X.; Niyogi, S.; Jha, N.; Haddon, R. C. Hexahapto-Metal Complexes of Single-Walled Carbon Nanotubes. *Macromol. Chem. Phys.* **2012**, *213*, 1001–1019.
- (21) Moser, M. L.; Tian, X.; Pekker, A.; Sarkar, S.; Bekyarova, E.; Itkis, M. E.; Haddon, R. C. Hexahapto-Lanthanide Interconnects Between the Conjugated Surfaces of Single-Walled Carbon Nanotubes. *Dalton Trans.* **2014**, *43*, 7379–7382.
- (22) Moser, M. L.; Pekker, A.; Tian, X.; Bekyarova, E.; Itkis, M. E.; Haddon, R. C. Effect of Lanthanide Metal Complexation on the Properties and Electronic Structure of Single-Walled Carbon Nanotube Films. *ACS Appl. Mater. Interfaces* **2015**, *7*, 28013–28018.
- (23) Li, E. Y.; Marzari, N. Improving the Electrical Conductivity of Carbon Nanotube Networks: A First-Principles Study. *ACS Nano* **2011**, *5*, 9726–9736.
- (24) Avdoshenko, S. M.; Ioffe, I. N.; Cuniberti, G.; Dunsch, L.; Popov, A. A. Organometallic Complexes of Graphene: Toward Atomic Spintronics Using a Graphene Web. ACS Nano 2011, 5, 9939—9949.
- (25) Dai, J.; Zhao, Y.; Wu, X.; Zeng, X. C.; Yang, J. Organometallic Hexahapto-Functionalized Graphene: Band Gap Engineering with Minute Distortion to the Planar Structure. *J. Phys. Chem. C* **2013**, *117*, 22156–22161.
- (26) Ketolainen, T.; Havu, V.; Puska, M. J. Enhancing Conductivity of Metallic Carbon Nanotube Networks by Transition Metal Adsorption. *J. Chem. Phys.* **2015**, *142*, 054705.
- (27) Gloriozov, I. P.; Marchal, R.; Saillard, J.-Y.; Oprunenko, Y. F. Chromium Tricarbonyl and Chromium Benzene Complexes of Graphene, Their Properties, Stabilities, and Inter-Ring Haptotropic Rearrangements A DFT Investigation. *Eur. J. Inorg. Chem.* **2015**, 2015, 250–257.
- (28) Sarkar, S.; Zhang, H.; Huang, J.-W.; Wang, F.; Bekyarova, E.; Lau, C. N.; Haddon, R. C. Organometallic Hexahapto Functionalization of Single Layer Graphene as a Route to High Mobility Graphene Devices. *Adv. Mater.* **2013**, *25*, 1131–1136.
- (29) Tian, X.; Sarkar, S.; Moser, M. L.; Wang, F.; Pekker, A.; Bekyarova, E.; Itkis, M. E.; Haddon, R. C. Effect of Group 6 Transition Metal Coordination on the Conductivity of Graphite Nanoplatelets. *Mater. Lett.* **2012**, *80*, 171–174.
- (30) Tian, X.; Moser, M. L.; Pekker, A.; Sarkar, S.; Ramirez, J.; Bekyarova, E.; Itkis, M. E.; Haddon, R. C. Effect of Atomic

Interconnects on Percolation in Single-Walled Carbon Nanotube Thin Film Networks. *Nano Lett.* **2014**, *14*, 3930–3937.

- (31) Biswas, S.; Drzal, L. T. A Novel Approach to Create a Highly Ordered Monolayer Film of Graphene Nanosheets at the Liquid-Liquid Interface. *Nano Lett.* **2009**, *9*, 167–172.
- (32) Lotya, M.; Hernandez, Y.; King, P. J.; Smith, R. J.; Nicolosi, V.; Karlsson, L. S.; Blighe, F. M.; De, S.; Wang, Z. M.; McGovern, I. T.; Duesberg, G. S.; Coleman, J. N. Liquid Phase Production of Graphene by Exfoliation of Graphite in Surfactant/Water Solutions. *J. Am. Chem. Soc.* 2009, 131, 3611–3620.
- (33) Sun, X.; Ramesh, P.; Itkis, M. E.; Bekyarova, E.; Haddon, R. C. Dependence of the Thermal Conductivity of Two-Dimensional Graphite Nanoplatelet-Based Composites on the Nanoparticle Size Distribution. *J. Phys.: Condens. Matter* **2010**, *22*, 334216.
- (34) Biswas, S.; Fukushima, H.; Drzal, L. T. Mechanical and electrical property enhancement in exfoliated graphene nanoplatelet/liquid crystalline polymer nanocomposites. *Composites, Part A* **2011**, *42*, 371–375.
- (35) Pekker, A.; Chen, M.; Bekyarova, E.; Haddon, R. C. Photochemical Generation of Bis-hexahapto Chromium Interconnects Between the Graphene Surfaces of Single-Walled Carbon Nanotubes. *Mater. Horiz.* **2015**, *2*, 81–85.
- (36) Vanier, N. Properties of Plasma Produced Graphene Nanonplatelets and Electrical Conductivity Applications; IDTechEx: Santa Clara, CA, 2014.
- (37) Khan, U.; O'Neill, A.; Lotya, M.; De, S.; Coleman, J. N. High-Concentration Solvent Exfoliation of Graphene. *Small* **2010**, *6*, 864–871.
- (38) Lotya, M.; King, P. J.; Khan, U.; De, S.; Coleman, J. N. High-Concentration, Surfactant-Stablized Graphene Dispersions. *ACS Nano* **2010**, *4*, 3155–3162.
- (39) Niyogi, S.; Bekyarova, E.; Itkis, M. E.; Zhang, H.; Shepperd, K.; Hick, J.; Sprinkle, M.; Berger, C.; Lau, C. N.; de Heer, W. A.; Conrad, E. H.; Haddon, R. C. Spectroscopy of Covalently Functionalized Graphene. *Nano Lett.* **2010**, *10*, 4061–4066.
- (40) de Heer, W. A.; Berger, C.; Wu, X.; Sprinkle, M.; Hu, Y.; Ruan, M.; Stroscio, J.; First, P. N.; Haddon, R. C.; Piot, B.; Faugeras, C.; Potemski, M.; Moon, J.-S. Epitaxial Graphene Electronic Structure and Transport. *J. Phys. D: Appl. Phys.* **2010**, *43*, 374007.
- (41) Tian, X.; Sarkar, S.; Pekker, A.; Moser, M. L.; Kalinina, I.; Bekyarova, E.; Itkis, M. E.; Haddon, R. C. Optical and Electronic Properties of Thin Films and Solutions of Functionalized Forms of Graphene and Related Carbon Materials. *Carbon* **2014**, *72*, 82–88.
- (42) Kalinina, I.; Bekyarova, E.; Wang, Q.; Al-Hadeethi, Y. F.; Zhang, X. J.; Al-Agel, F.; Al-Marzouki, F.; Yaghmour, S.; Haddon, R. C. Formation of Transition Metal Cluster Adducts on the Surface of Single-Walled Carbon Nanotubes: HRTEM Studies. Fullerenes, Nanotubes, Carbon Nanostruct. 2014, 22, 47–53.
- (43) Kalinina, I.; Al-Hadeethi, Y. F.; Bekyarova, E.; Zhao, C.; Wang, Q.; Zhang, X.; Al-Zahrani, A.; Al-Agel, F.; Al-Marzouki, F.; Haddon, R. C. Solution-phase Synthesis of Chromium-functionalized Single-Walled Carbon Nanotubes. *Mater. Lett.* **2015**, *142*, 312–316.
- (44) Novoselov, K. S.; Geim, A. K.; Morozov, S. V.; Jiang, D.; Zhang, Y.; Dubonos, S. V.; Grigorieva, I. V.; Firsov, A. A. Electric Field Effect in Atomically Thin Carbon Films. *Science* **2004**, *306*, 666–669.
- (45) Lin, W. H.; Chen, T. H.; Chang, J. K.; Taur, J. I.; Lo, Y. Y.; Lee, W. L.; Chang, C. S.; Su, W. B.; Wu, C. I. A Direct and Polymer-free Method for Transferring Graphene Grown by Chemical Vapor Deposition to Any Substrate. *ACS Nano* **2014**, *8*, 1784–1791.